

Effect of a Bacterial Consortium on Passivation Property of 2024 Aluminum Alloy

Daniel Ortega¹, Claudia Alvarado¹, Lisa Muñoz², Hans Kohler³, Fabiola Pineda⁴, Maritza Páez², Mamie Sancy⁴, Nelson D. Vejar¹ and Jenny M. Blamey^{2,3,*}

¹ Academia Politécnica Aeronáutica, Fuerza Aérea de Chile, Av. José Miguel Carrera 11087, El Bosque, Santiago, Chile.

² Facultad de Química y Biología, Universidad de Santiago de Chile, Alameda 3363, Estación Central, Santiago, Chile

³ Fundación Biociencia, José Domingo Cañas 2280, Ñuñoa, Santiago, Chile.

⁴ Escuela de Construcción Civil, Facultad de Ingeniería, Pontificia Universidad Católica de Chile. Av. Vicuña Mackenna 4860, Santiago, Chile.

*E-mail: jblamey@bioscience.cl

Received: 23 May 2018 / Accepted: 28 September 2018 / Published: 5 January 2019

A bacterial consortium was recollected from corrosion products formed on a vertical fin of a military helicopter exposed to Antarctic environment for 4 years. For the identification and characterization of the consortium, DNA sequencing was performed showing that the consortium was mainly composed by three strains. Two of the strains showed a close affiliation to *Bacillus toyonensis* and *Staphylococcus aureus*. However, the third strain studied did not show affiliation by 16S rRNA analysis to any genus so far described. Additionally, morphological and electrochemical studies of an aluminum 2024-T3 alloy prior and after exposure to a sterile and inoculated minimal salt medium at 4 °C were carried out by using scanning electron microscope, open circuit potential and electrochemical impedance spectroscopy. The experimental results revealed that steady-state properties of the passive film were modified by the bacterial consortium and isolates.

Keywords: Antarctica, aluminum alloy, 2024-T3, consortium, *Bacillus toyonensis*, *Staphylococcus aureus*

1. INTRODUCTION

Preliminary studies carried out in Antarctica have revealed corrosion of passive alloys even though temperature and humidity parameters measured had lower values than those reported as critical by the literature, regarding corrosion of metallic materials. It is worth to mention that corrosion processes are triggered when environmental factors as salinity, temperature, pH, relative humidity and

levels of radiation (UV) are high. This indicates there are other factors influencing the corrosion process. One of these determining factors may be the presence of microorganisms, which are adapted to the extreme environment present in Antarctica. In addition, anaerobic heterotrophic and aerobic bacteria as well as sulfate reducing bacteria, fungi and yeasts have been found in samples taken from corroded sites in different airplanes [1]. For instance, a microbial community was found in fuel tanks manufactured with AA2024-T3, containing jet propellant-8 (JP-8) [2]. Isolated cultures were closely related to the genus *Bacillus* and to the fungi *Aureobasidium* and *Penicillium* influencing the electrochemical results revealing corrosion of the metallic surface [3]. Investigations about corrosion of AA2024 in the presence of the hydrocarbon-degrading bacteria *Bacillus cereus* ACE4 (a Gram-positive bacteria) and *Serratia marcescens* ACE2 (a Gram-negative bacteria) expose to a fuel tank simulated environment showed pitting corrosion damage caused by *B. cereus* ACE4, being more vigorous compared to that from *S. marcescens* ACE2. This could be associated to the higher capacity of adhesion from *B. cereus* ACE4 due to cell surface hydrophobicity [4]. In addition, AA2024-T3 exposed to bacteria *Bacillus subtilis* in minimal salt medium (MSM) solution has also shown evidence of corrosion after one month of immersion in this medium, determined by electrochemical measurements [5].

In this work, we study a corrosion phenomenon detected in a vertical fin of a military helicopter exposed for 4 years to the environmental conditions present in the Antarctic continent. Samples of corrosion products were collected from this component. The corrosion products were analyzed by chemical and microbiological techniques. Cultures revealed the presence of three strains belonging to the genera *Bacillus*, *Staphylococcus* and third one to an unknown genus not described in the data bases. Electrochemical measurements and morphological analysis of AA2024-T3 specimens exposed to sterile and inoculated media indicate that one of these isolated bacteria influenced the evolution of the passive film.

2. EXPERIMENTAL METHODS

2.1. Metallic Substrates

To carry out the experimental studies, the Chilean aerospace company ENAER provided testing aluminum alloy AA2024-T3 specimens, sized 100×100×2 mm, with nominal chemical composition: (wt.%) 92.400 Al, 4.900 Cu, 1.520 Mg, 0.169 Fe, 0.520 Mn, 0.080. The specimens were degreased using a trichloroethylene solution at 90°C for 5 min, followed by an anodizing process using Turco 4215-S solution at 54°C for 15 min with stirring. Later, washing was done with bi-distilled water at room temperature and a pickling cleaning surface treatment was performed by using the industrial reagent Smut Go N°4 deoxidizer (30–45 g/l of 10% HNO₃) at room temperature for 10 min with stirring. Washing was again done with bi-distilled water at room temperature. The chromic acid anodizing (CAA) process was carried out using an electrolyte with following containing: 50g/L of H₂CrO₄, 0.5 g/L of Na₂SO₄, 0.2 g/L of NaCl, and a current density of 5 mA/cm² for 30 min at 35°C [6,7].

2.2. Sample Collection and Bacterial Strains

Samples of corrosion products were obtained from a vertical fin of a military helicopter located in a Chilean Antarctic Air Base (marine environment). The corrosion products were stored in sterile plastic receptacles (Zelle, Germany). Samples were transported in a cooler packed with ice to maintain the integrity of the sample. Microorganisms present in the samples conforming a consortium were cultivated and then isolated by serial dilutions and solid media plating in Luria Bertani Broth medium (LB) composed of (per L): 10 g tryptone, 5 g yeast extract, and 10 g NaCl. The bacterial consortium and isolated strains were stored at $-20\text{ }^{\circ}\text{C}$ to ensure the purity and consistency of the microbial material through all subsequent experiments.

2.3. Microbiological and Biochemical characterization

Gram stain

Gram stain reaction was carried out using a Merck gram stain kit (Cat # 111885), according to the manufacturers recommended protocol.

Scanning electron microscopy of microorganisms

For Scanning Electron Microscopy (SEM), cells were concentrated by centrifugation and then fixed 16 h in 3% V/V glutaraldehyde in phosphate buffer. They were filtered using a polyamide filter (Sartorius) with a porous size of $0.45\text{ }\mu\text{m}$. The fixed cells were dehydrated by sequential passage through increased concentrations of ethanol (50-100% V/V) in 10% increments, dried with liquid CO_2 in a critical point dryer, and then coated with gold - palladium for 60s. Samples were visualized using an electronic microscope Hitachi TM3000 with a beam voltage of 15kVolts.

Molecular Bacterial identification

The 16S rDNA gene of three different microbial strains, named subsequently B-A, B-B and B-C, was amplified from genomic DNA by PCR (Polymerase Chain Reaction) using primers 515F [8] specific for Bacteria, and the universal primer 1492R [9]. The reaction mix was formed using $0.25\text{ }\mu\text{L}$ of Taq DNA polymerase (500 U/mL), $5\text{ }\mu\text{L}$ of each deoxy (d) nucleotide (2 mM) (dATP, dCTP, dGTP and dTTP; deoxyadenosine triphosphate, deoxycytidine triphosphate, deoxyguanosine triphosphate and deoxythymidine triphosphate), $5\text{ }\mu\text{L}$ of buffer, $4\text{ }\mu\text{L}$ of MgCl_2 (0.75 mM) and $0.5\text{ }\mu\text{L}$ of each primer (100 mM). The following thermal conditions were applied: $95\text{ }^{\circ}\text{C}$ for 45 s, $55\text{ }^{\circ}\text{C}$ for 45 s, $72\text{ }^{\circ}\text{C}$ for 45 s. Each cycle was repeated thirty times and a final elongation step of $72\text{ }^{\circ}\text{C}$ for 10 min was added. Amplification reactions were carried out using a Palm Gradient Cycler (PCR) (Corbett). Verification of PCR amplifications was carried out by running the sample on a 1.5% agarose gel stained with SYBR gold (Invitrogen). The obtained sequences were assembled, analyzed, and manually edited

using Chromas Pro software (Technelysium Pty Ltd.). Strains were taxonomically classified using the Naïve Bayesian rRNA Classifier function from the RDP-Ribosome Database Project [10].

Screening of enzyme activities

Activity for several enzymes was studied using a semi-quantitative method for detection of enzymatic activities (Kit API 20E, BioMerieux) and analyzed using Bergey's Manual of Bacteriology [11,12]. A pure broth culture was prepared and centrifuged at 13000 rpm to prepare a suspension which was later re-suspended on an isotonic medium, prior the detection of enzymatic activities. All assays were carried out at 15 °C.

2.4. Development of biofilms and corrosion in an aerated inoculated medium

The metallic alloy AA2024-T3 plates were exposed to UVC germicidal light in a laminar flow hood to sterilize them for 15 min per side. The same procedure was implemented for the material used in all the experiments. For the electrochemical studies, an electrochemical cell was used containing media with the different inoculum. The sterile culture medium utilized was MSM, which contained (per L): 0.22 g of $(\text{NH}_4)_2\text{SO}_4$, 1.20 g of KH_2PO_4 , 0.23 g of $\text{MgSO}_4 \cdot 7\text{H}_2\text{O}$, 0.25 g of CaCl_2 , and 0.024 g of yeast extract [13]. In addition, 0.3 mL of strains B-A, B-C and B-B grown in LB were cultured in MSM at -4 °C (1/100 mL) overnight in order to mimic the Antarctic conditions. The culture was inoculated (10^8 CFU/mL) on the electrochemical cell containing an AA2024-T3 plate, as working electrode, at the bottom of the electrochemical cell. To maintain bacterial density near the steady state growth phase throughout the experiment, a semi-continuous mode of culture growth was employed. The cultures were maintained in the cell to observe the development of biofilm along with corrosion.

2.5 Electrochemical Measurements

The electrochemical measurements were registered with a VSP 200 Bi-potentiostat (Biologic, USA) at 4 ± 2 °C. The experiments were performed in a three-electrode electrochemical cell. The working electrode was an AA2024-T3 sample and the area for it was 21 cm². Prior to perform the electrochemical tests the samples were sterilized with alcohol, washed with distilled water and exposed to UV light for 15 min. The same procedure was implemented for the all material used in the experiments. A large platinum grid was used as the counter electrode. The potentials were referenced to a KCl saturated calomel electrode (SCE).

The control electrolyte used consisted of 100 mL of minimum salt media (MSM), that contained (per L): 0.22 g of $(\text{NH}_4)_2\text{SO}_4$, 1.20 g of KH_2PO_4 , 0.23 g of $\text{MgSO}_4 \cdot 7\text{H}_2\text{O}$, 0.25 g of CaCl_2 , and 0.024 g of yeast extract [8]. In addition, 0.3 mL of *B. toyonensis*, *S. aureus* and unknown strain B-B grown in LB were cultured in MSM at -4 °C (1/100 mL) overnight in order to mimic the Antarctic conditions. The cultures were inoculated (10^8 CFU/mL) on the electrochemical cell, containing AA2024-T3 alloy piece as working electrode at the bottom of the electrochemical cell. To maintain

bacterial density near the steady state growth phase throughout the experiment a semi-continuous culture growth was employed, i.e. 75% of the medium was drained and replaced with an equal amount of fresh sterile medium every 48h. As the cultures grew we observed the development of biofilm. For each sample studied, 1 mL of the respective bacterial strain was added to MSM media.

The measurements were performed in triplicate to ensure reproducibility and were tested different times of exposure for the bacterial strain to the metallic surface. Electrochemical impedance spectroscopy (EIS) measurements were obtained at open circuit potential as a function of immersion time, using a sinusoidal signal with 10 mV as amplitude over frequencies ranging from 100 kHz to 3 mHz.

2.6 Morphological analysis

Two different types of microscopes were used for morphological studies. First it was used a phase contrast microscope (Nikon Eclipse 80i). Pictures were taken from dilutions of the cultures under study from a 10^{-3} dilution. Then, a scanning electron microscope (JEOL, model JSM-6010LA) with a beam voltage of 14-15 kV was used to visualize the morphology of the AA2024-T3 surface expose to sterile and inoculated media. The microorganisms at a concentration of $\sim 10^8$ CFU/ml measured at 600 nm were inoculated on the coupons. The bacterial strain on the coupons were then fixed for 45min in a 2.5% glutaraldehyde solution at 4 °C. Later, the samples were dehydrated using an increasing ethanol concentration solutions (25, 50 and 75%) for 15 min [14].

The metal surface topography of the coupons and elemental composition were examined after removal of biofilms formed on the metallic surface using ethanol and an ultrasonic device (Elma, model S3) for 15 min, before subjecting the coupons to SEM-EDAX analyses.

3. RESULTS

3.1 Microbiological analysis

Three different microbial strains were separated and isolated from the Antarctic microbial consortium by serial dilutions and plating techniques. Colonies were picked, cultivated and the isolates were initially named as B-A, B-B, and B-C. Cells of the microorganism B-A were approximately 4 μm long and 0.75 μm in diameter, while the novel *Bacillus B-B*, described has cells of approximately 2 μm long and 0.5 μm in diameter. Meanwhile the third microorganism is of spherical shape of diameter of 1 μm (Fig. 1).

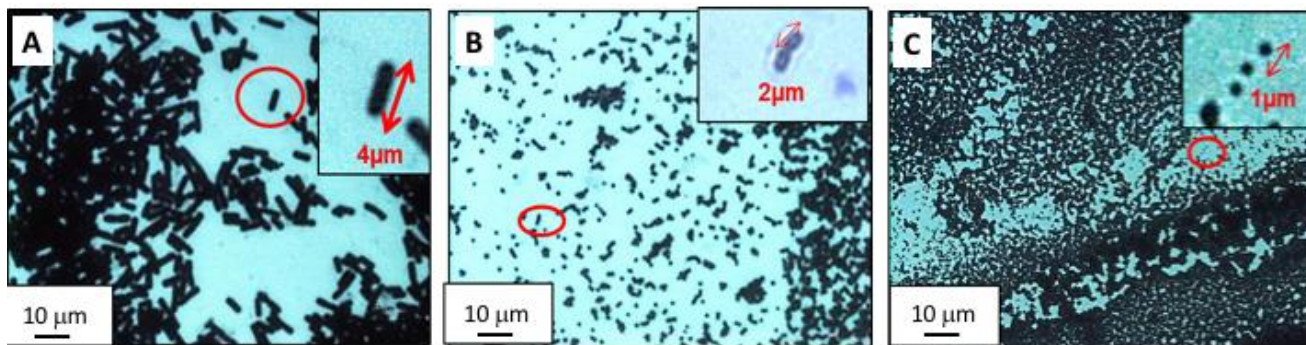


Figure 1. Optical Microscopic pictures of three microorganisms present in the biocorrosion consortium: (a) *Bacillus toyonensis*, (b) *Bacillus* not previously described (B-B) and (c) *Staphylococcus aureus*.

The Gram test identified microorganism B-A as Gram positive and microorganisms B-B and B-C as Gram negative. The 16S rDNA sequence analysis was used to further identify the bacterial strains. This analysis identified strain B-A as member of *Bacillus* genera, with a very close affiliation to *Bacillus toyonensis*. Similarly, strain B-C was identified as member of the genera *Staphylococcus* with a very close affiliation to *Staphylococcus aureus*. However, one of the microorganism cultivated, bacterial strain B-B, did not show any affiliation to already described genus in the literature, based on the 16S rDNA analysis. In this work, this strain is referred as B-B (see Table 1).

Table 1. Identification of the isolated microorganisms present in the 2024-T3 Antarctic microbial consortium.

Sample	Microorganism	Identity (%)
B-A	<i>Bacillus toyonensis</i> BCT-7112	99%
B-B	Unknown microorganism	not identified
B-C	<i>Staphylococcus aureus</i> subsp. aureus N315	99%

Table 2. Biochemical comparison of microorganism B-B and *Bacillus subtilis* using API 20E STREP.

Test	<i>Bacillus subtilis</i>	Microorganism B-B
β-galactosidase	d	+
Arginine dehydrolase	-	+
Lysine decarboxilase	-	-
Utilization Trisodium Citrate	+	+
Production of H ₂ S	-	+
Urease	-	-
Tryptophan deaminase	-	-
Indole production	-	+
Gelatinase	+	+
Glucose -Fermentation-Oxidation	+	+
Nitrite production	+	+

d corresponds to a 11 – 89% of *B. subtilis* strains that show + reaction for β-galactosidase according to the Bergey’s Manual.

Additionally, B-B bacterial strain was analyzed by API 20E STREP Kit to perform a biochemical characterization. Results were compared with information found in the Bergey's Manual (Table 2). This microorganism showed a different enzymatic biochemical profile when compared with *Bacillus subtilis* (Table 2). After this analysis, results support the idea that this microorganism is a novel bacterial strain isolated from the Antarctic consortium and may play a role in the corrosion process.

3.2 Electrochemical behavior

Figure 2 shows the variation of the open circuit potential (E) of AA2024-T3 after being exposed to sterile and inoculated MSM as a function of immersion time. As can be seen, in the sterile and inoculated MSM with the consortium, the open circuit potential value was slightly shifted to more negative values with immersion time, which might indicate a slight increase of the corrosion current. On the other hand, for the inoculated media with *S. aureus*, *Bacillus* not previously described (B-B) and *B. toyonensis*, the open circuit potential value was also slightly shifted with immersion time, but at both positive and negative values. For inoculated media with *B. toyonensis* after day 60 the open circuit potential value was shifted from -0.51 to -0.45 V vs SCE, that might indicate a slight decrease of the corrosion current.

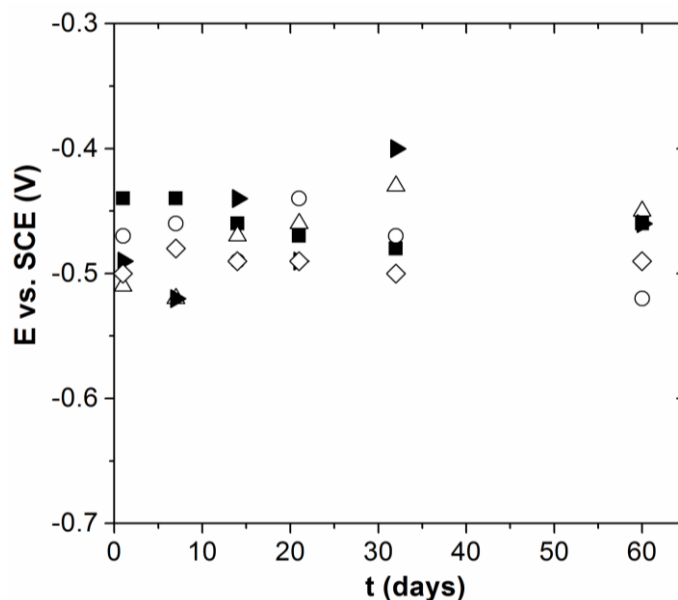


Figure 2. Variation of open circuit potential values of AA2024-T3 after day 60 of exposure in MSM (■) sterile and inoculated with (◇) consortium, (○) *S. aureus*, (△) *B. toyonensis* and (▴) B-B at 4 °C. Electrode surface Area = 21 cm² and $E = E_{OCP}$.

Figure 3 shows the EIS diagrams for AA2024-T3 after day 21 and 60 of immersion time in sterile and inoculated MSM. For all media, a capacitive behavior was observed which was characterized by a single time constant related to a passive oxide film formed on the metal surface. In addition, the impedance responses reveal clearly the existence of potential and current distribution. This might indicate the formation of corroded areas in the oxide film/aluminum surface that might be

associated to the chemical and biological reactions resulting from the biofilms formation, which may be associated to a CPE behavior, as it was described previously in Ref [2,7,15,16]. On the other hand, the impedance modulus of AA2024-T3 after day 21 of immersion in sterile medium was lower than the inoculated media at all frequency. Nevertheless, the impedance modulus of AA2024-T3 after day 60 of immersion in sterile medium was also the same that in inoculated media with *S. aureus* but greater than in inoculated media with B-B and *B. toyonensis*.

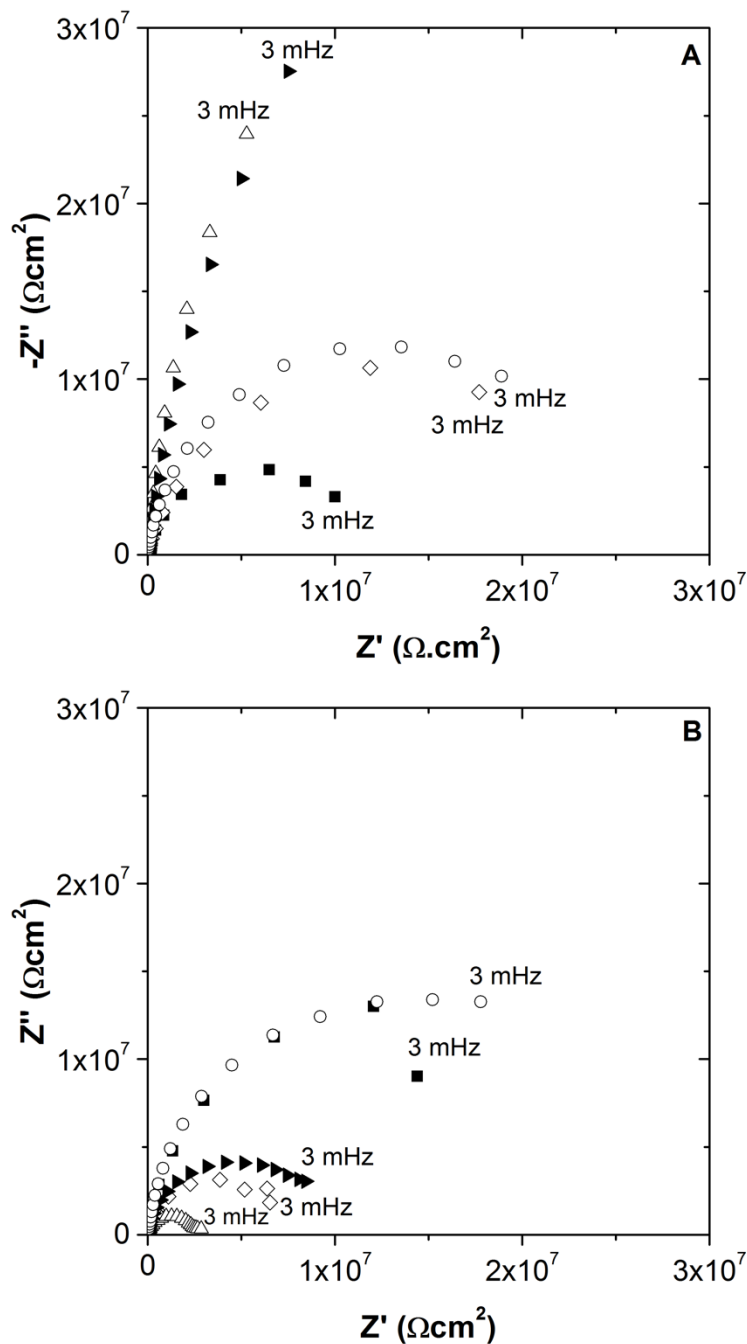


Figure 3. Nyquist diagram of AA2024 after day 21 and 60 of exposure in MSM (■) sterile and inoculated with (◇) consortium, (○) *S. aureus*, (△) *B. toyonensis* and (►) B-B at 4 °C and open circuit potential condition. Electrode surface Area = 21 cm².

Note that the impedance modulus at low frequency range may be associated with the oxide resistance. Recently, Alvarado [2] showed a slight increase of the impedance modulus at 5 mHz ($|Z|_{f=5 \text{ mHz}}$) with time for AA2024-T3 after being exposed to a media containing jet JP-8 and a microbial community recollected from corrosion products. As can be seen in Table 3, for all media the impedance modulus at 3 mHz ($|Z|_{f=3 \text{ mHz}}$) decreased with time, which might reveal a slight increase of the anodic current.

Table 3. Impedance parameters obtained of AA2024-T3 samples in sterile and inoculated media after day 21 and 60 by using numerical analysis.

System	t_{exp} (days)	$ Z _{f=3 \text{ mHz}}$ (Ωcm^2)	α	Q ($\Omega^{-1}\text{s}^{\alpha}\text{cm}^{-2}$)
MSM Sterile	21	7.4×10^6	0.85	16.0×10^7
MSM Consortia		9.9×10^6	0.89	9.4×10^7
MSM/ <i>B. Toyonensis</i>		17.6×10^6	0.96	8.1×10^7
MSM /B		15.9×10^6	0.92	7.9×10^7
MSM/ <i>S. aureus</i>		12.1×10^6	0.91	9.2×10^7
MSM Sterile	60	0.1×10^6	0.89	9.2×10^7
MSM Consortia		5.7×10^6	0.88	10.6×10^7
MSM/ <i>B. toyonensis</i>		2.4×10^6	0.85	11.5×10^7
MSM /B		7.1×10^6	0.92	9.8×10^7
MSM/ <i>S. aureus</i>		0.1×10^6	0.89	8.9×10^7

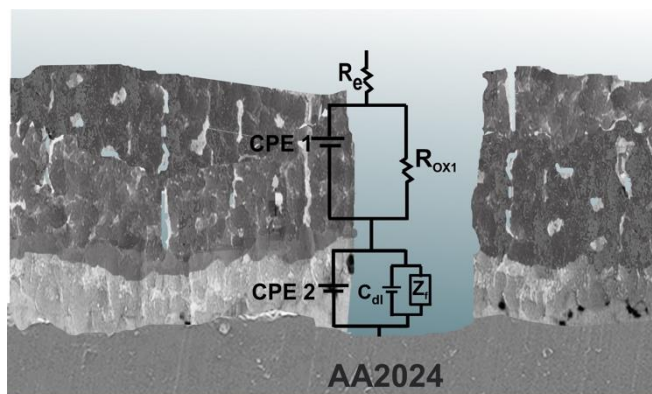


Figure 4. Schematic representation for coated 2024 alloy and corresponding equivalent circuit [16,17].

An equivalent circuit and schematic representation of alumina oxide film/2024 alloy interface is presented in Figure 4. In this case, R_e is the electrolyte resistance. The oxide film is composed by an outer layer that was formed during the anodizing process and an inner layer attributed to the natural oxide film. In addition, constant phase elements were introduced instead of pure capacitances in order to take into account the non-ideal behavior of the passive film. Paez [16,17] showed that the thickness of the outer oxide layer is thicker than the inner oxide layer, the resistance R_{ox} was only considered for

the outer oxide film. C_{dl} represents the double layer capacitance and Z_f is the Faradaic impedance, such as was described in Ref [4,18,19]. Note that the experimental data were perfectly fitted with the equivalent circuit and values of the parameters were extracted by graphic and numerical analysis. The CPE parameters are also showed in Table 3.

As it was described in Ref [19,20], from the impedance analysis the thickness of the oxide film formed on a metallic surface may be obtained by using the capacitance values. As shown Table 4, the thickness values are in agreement with those previously reported for passive layers by Alvarado [2] and Benoit [19]. In particular, the thickness of the oxide film increased slightly with time in sterile and inoculated MSM with the consortium, which is in agreement with the variation of the OCP with time. However, in inoculated media with *B. toyonensis*. B-B and *S. aureus*, the range of the thickness of the oxide film slightly decreased with time. This behavior might indicate that the anodic current slightly increased or that the oxide properties were modified.

Table 4. Impedance parameters obtained of AA2024-T3 samples in sterile and inoculated media after day 21 and 60 by using numerical analysis.

System	t_{exp} (days)	Thickness range (nm)
MSM Sterile	21	6.8 – 10.4
MSM Consortia		12.8 – 15.3
MSM/ <i>B. toyonensis</i>		11.9 – 13.6
MSM /B		10.8 – 13.6
MSM/ <i>S. aureus</i>		12.2 -14.9
MSM Sterile	60	10.4 – 13.2
MSM Consortia		9.9 – 12.9
MSM/ <i>B. toyonensis</i>		10.9 – 14.4
MSM /B		11.2 – 13.4
MSM/ <i>S. aureus</i>		10.4 – 13.2

Table 5. Corrosion parameters obtained from polarization curves of AA2024-T3 samples in sterile and inoculated media after day 21.

t_{exp} / days	System	I_a at $E = -0.395$ V / $A\ cm^{-2}$
21	MSM	3.26×10^{-7}
	MSM/ <i>B. toyonensis</i>	2.97×10^{-6}
	MSM/B-B	4.84×10^{-7}
	MSM/ <i>S. aureus</i>	2.13×10^{-6}

In order to better understand the oxide film properties, Figure 5 shows the polarization curves of AA 2024-T3 after day 21 of immersion in sterile and inoculated MSM media. The corrosion potential was shifted to more negative value in inoculated media, as it was revealed in the slightly variation of the open circuit potential with time (Fig. 3). Moreover, the anodic and cathodic currents

decreased in inoculated media. Nevertheless, if the anodic current is compared in the passive domain, for example at $E = 0.395$ vs. SCE (V), as shown Table 5, the anodic current increased from sterile to inoculated media for all isolated bacteria, which indicate that the oxide film properties might be modified by the biofilm formation.

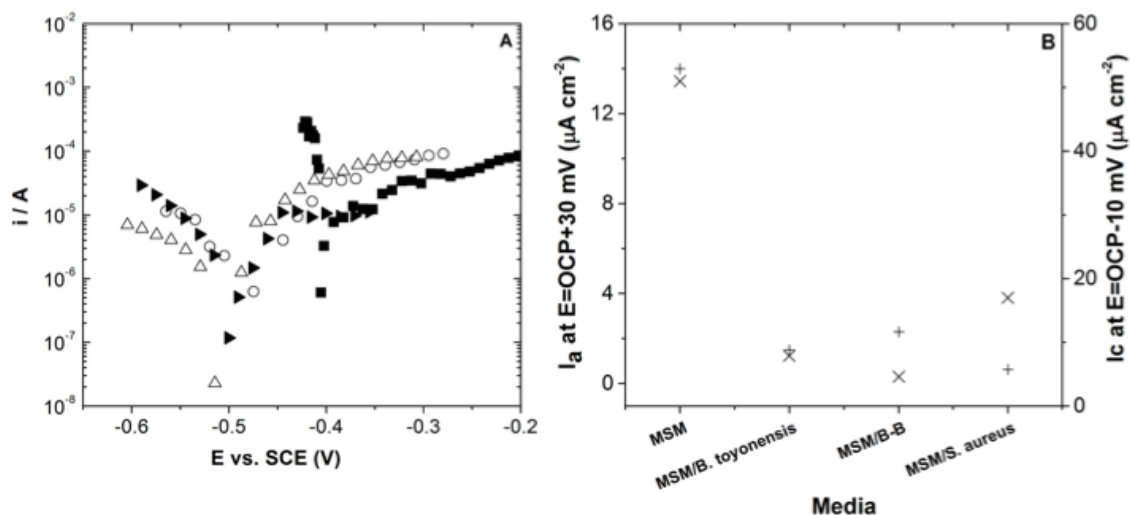


Figure 5. Polarization curves of AA 2024-T3 after 21 day of exposure in MSM (■) sterile, (○) *S. aureus*, (►) *B. B* and (△) *B. toyonensis*. Scan rate 0.1 mV s^{-1} and electrode surface Area = 21 cm^2 .

3.3 Morphological characterization of strains

Figure 6 shows SEM micrographs of AA2024 alloy surfaces after 7 days of exposure to sterile and inoculated media. The textured appearance of local surface regions may be associated to the presence of a biofilm generated by *B. toyonensis*. Cells of this microorganism are approximately $4 \mu\text{m}$ long and $0.75 \mu\text{m}$ in diameter, while the novel *Bacillus B-B*, described has cells of approximately $2 \mu\text{m}$ long and $0.5 \mu\text{m}$ in diameter. In the case of *S. aureus*, the cells were spherical with a diameter of $1 \mu\text{m}$. This figure also shows the EDX analysis along to the respective electron microscopy photograph, revealing the alumina oxide film on the AA2024-T3.

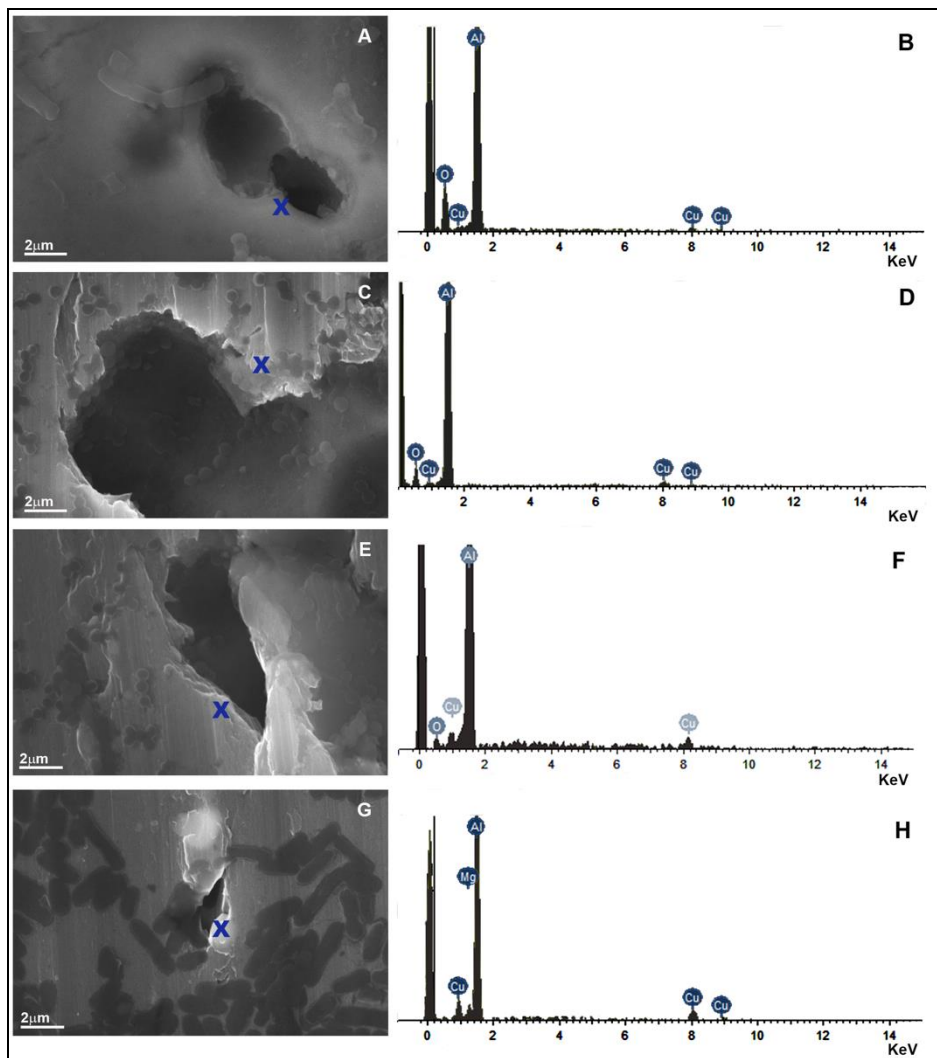


Figure 6. SEM/EDX analysis of AA2024-T3 alloy sample after to be exposed to (a,b) *B. toyonensis*, (c,d) *S. aureus* (e,f) consortium and (g,h) *Bacillus* not previously described (B-B).

4. CONCLUSIONS

The corrosion phenomena detected in a vertical fin of a military helicopter exposed for 4 years to the environmental conditions present in the Antarctic continent and exposed permanently to extreme Antarctic conditions showed that the process of metallic deterioration is not only due to the effect of abiotic environmental conditions proper of the Antarctic continent. The microorganisms in the corroded samples taken from the vertical fin of the mentioned helicopter contribute to the alteration of the corrosion process of the AA2024-T3. Three main microorganisms were detected in the isolated consortium. Through the analysis of 16S rDNA it was possible to identify the cultured microorganisms as *B. toyonensis*, for microorganism B-A, *S. aureus* for microorganism B-C, meanwhile the newly isolated microorganism B-B did not show any affiliation to the already described species present in the literature so far. Further biochemical and metabolic studies are required in order to fully characterize this new microorganism.

The experimental electrochemical results revealed that when in contact with AA2024-T3 alloy, the microorganisms described above, and the consortium formed by them modify the electrochemical behavior of the aluminum alloy as a function of immersion time, changing the passive oxide film properties formed on the AA2024-T3 surface. This behavior may be attributed to the influence on the dissolution/formation reaction of the aluminum oxide layer by the presence of the microorganisms and their metabolic products, exerting an influence on the corrosion development process. However, no information has been found on the direct relationship between the interactions of these variables. Additional analysis and studies are needed in order to better understand the interaction of these microorganisms individually and as a consortium with the metallic surface.

ACKNOWLEDGEMENTS

The authors also would like to thank to the following agencies: AFOSR (Grant FA9550-14-1-0407), PIA-Conicyt (Grant ACT-1412), Fondecyt (Grant 1160604 and 11170419).

References

1. A. Hagenauer, R. Hilpert, T. Hack, *Mater. Corros.*, 45 (1994) 355.
2. C. Alvarado, M. Sancy, J.M. Blamey, C. Galarce, A. Monsalve, F. Pineda, N. Vejar, M. Páez, *Electrochim. Acta*, 247 (2017) 71.
3. C. McNamara, T. Perry, R. Leard, K. Bearce, J. Dante, R. Mitchell, *Biofouling*, 21 (2005) 257.
4. A. Rajasekar, B. Anandkumar, S. Maruthamuthu, Y.P. Ting, P.K.S.M. Rahman, *Appl. Microbiol. Biotechnol.*, 85 (2010) 1175.
5. A. Monsalve, M. Páez, M. Toledano, A. Artigas, Y. Sepúlveda, N. Valencia, *Eng. Mater. Struct.*, 30 (2007) 748.
6. A.N. Khramov, V.N. Balbyshev, N.N. Voevodin, M.S. Donley, *Prog. Org. Coatings*, 47 (2003) 207.
7. M. Sancy, A. Abarzúa, M.I. Azócar, J.M. Blamey, F. Boehmwald, G. Gómez, N. Vejar, M. Páez, *J. Electroanal. Chem.*, 737 (2015) 212.
8. M.A. Tanner, C.L. Everett, W.J. Coleman, M.M. Yang, D.C. Youvan, *Biotechnol. Alia.*, 8 (2000) 1.
9. Q. Wang, G.M. Garrity, J.M. Tiedje, J.R. Cole, *Appl. Environ. Microbiol.*, 73 (2007) 5261.
10. A. Rajasekar, Y.P. Ting, *Ind. Eng. Chem. Res.*, 49 (2010) 6054.
11. E. Gruner, A. von Graevenitz, M. Altwegg, *J. Microbiol. Methods*, 16 (1992) 101.
12. A.C. Vieira, A.R. Ribeiro, L.A. Rocha, J.P. Celis, *Wear*, 261 (2006) 994.
13. B.H. Sen, B. Piskin, T. Demirci, B.H. Sen, *Endod. Dent. Traumatol.*, 11 (1995) 6.
14. S. Baeza, N. Vejar, M. Gulppi, M. Azocar, F. Melo, A. Monsalve, J. Pérez-Donoso, C.C. Vásquez, J. Pavez, J.H. Zagal, X. Zhou, G.E. Thompson, M.A. Páez, *Corros. Sci.*, 67 (2013) 32.
15. A.K. Mishra, R. Balasubramaniam, *Corros. Sci.*, 49 (2007) 1027.
16. S. V. Lamaka, M.L. Zheludkevich, K.A. Yasakau, M.F. Montemor, M.G.S. Ferreira, *Electrochim. Acta.*, 52 (2007) 7231.
17. M.A. Páez, T.M. Foong, C.T. Ni, G.E. Thompson, K. Shimizu, H. Habazaki, P. Skeldon, G.C. Wood, *Corros. Sci.*, 38 (1996) 59.
18. M.A. Paez, O. Bustos, G.E. Thompson, P. Skeldon, K. Shimizu, G.C. Wood, *Film*, 147 (2000) 1015.
19. M. Benoit, C. Bataillon, B. Gwinner, F. Miserque, M.E. Orazem, C.M. Sánchez-Sánchez, B.

Tribollet, V. Vivier, *Electrochim. Acta.* 201 (2016) 340.

20. M. E. Orazem, B. Tribollet, *Electrochemical Impedance Spectroscopy*. Wiley, (2017) New Jersey, USA.

© 2019 The Authors. Published by ESG (www.electrochemsci.org). This article is an open access article distributed under the terms and conditions of the Creative Commons Attribution license (<http://creativecommons.org/licenses/by/4.0/>).